

Glucose Metabolic Reprogramming in Cancer Microenvironment

Ze Zhang

Jilin University

Nan Lin

Jilin University

Xingwang Zhang

Jilin University

Zihui Meng (✉ zhmeng@jlu.edu.cn)

Jilin University

Research Article

Keywords: Glucose Metabolism Enzyme, Energy Metabolic Reprogramming, Warburg Effect, Immune

Posted Date: April 27th, 2021

DOI: <https://doi.org/10.21203/rs.3.rs-438551/v1>

License: © ⓘ This work is licensed under a Creative Commons Attribution 4.0 International License.

[Read Full License](#)

Abstract

Background: Energy metabolism reprogramming (EMR) exerts a critical role in tumor progression and activation of tumor-associated immune cells. Understanding the structural changes upon metabolic networks of both cancer cells and immune settings is vital for the potential and effective incorporation of metabolism-targeted therapeutics clinically.

Methods: In the present study, we used 33 tumor types' transcriptome data from TCGA & UCSC and proteomic data from CPTAC to elaborate the EMR under the "Warburg Effect" in cancer. We assessed the role of metabolic enzymes in prognosis by redrawing the metabolic network and proportional hazards model (Cox) analysis. Based on machine learning, we identified determinants of tumor immune subtypes and used a scoring scheme for the correlation between immune cell infiltration and metabolic enzymes. Considering the immunophenotype relationship, we illustrated a novel bioinformatics horizontal alignment method.

Results: Systematic profiling of EMR would shed light on the common and divergent metabolic characteristics between tumor cells as well as the tumor-associated microenvironment, and whether the metabolic characteristics of these cells remain stable or change in course of tumor progression, indicating metabolic plasticity.

Conclusions: This article reviewed the recent understanding of metabolic changes in tumor progression and tumor-associated microenvironment' phenotype and function, which could help clinical doctors to understand EMR in tumor progression and treatment resistance.

Introduction

Since the proposal of the "Warburg effect" by a German scientist Warburg in the early years of the 19th century¹, the structural differences between metabolic networks of tumor cells and normal cells are becoming more attractive for biochemists^{2,3}. Since the advances in both gene sequencing and protein mass spectrometry technology, forming an emerging research field, gluconic metabonomics^{4,5}. Meanwhile, immune cells infiltrating the tumor microenvironment showed the characterization of multi-dimensional maps of metabolic structural changes by the unique composition of metabolic flows. Wherein research on glucose metabolism is the most profoundly. As mechanisms behind the involvement of glucose metabolism in tumor occurrence & development and immune cell infiltration have been elucidated, along with a better understanding of glucose, amino acid, and lipid metabolic networks, other researchers put forward with the "Post-Warburg effect"⁶. Up to the present, although researchers are extremely familiar with the basic knowledge frame of glucose metabolism and there are voluminous studies of related metabolic enzymes and their encoding genes⁷, the more intricate metabolic networks perplex the identification of key targets optimal for interventions⁸. Relative studies often concentrate on a single enzyme or the nearby upstream or downstream pathways to investigate changes in the metabolic flux and speculate possible alternations in metabolic networks as a whole by measuring expression

changes in metabolic substrates or products⁹. Although these studies have demonstrated the regulatory mechanisms of controlling glucose metabolism in various proliferative and non-proliferative cells via revealing changes in metabolic demands¹⁰, gain-of-function mutations in tumor cells, and structural alternations, such as mutations of regulatory elements of genes in the receptor promoter¹¹, alternative splicing of encoding genes^{12,13}, and isozyme replacement¹⁴, can help glucose metabolism out of dependence on growth factors physiologically¹⁵. Recent studies demonstrated the fact that the single control of some links in the glucose metabolism in tumor cells, including knockdown of mitochondrial pyruvate carrier (MPC)¹⁶, knockdown of the tricarboxylic acid (TCA)-cycle enzymes to reduce the activity¹⁷, or a shift in PKM2 to PKM1 by alternative splicing⁶, can obtain satisfactory outcomes in in vitro experiments with interventions¹⁸. However, in real patients, tumor cells obtain nutrients and restore metabolism already being inhibited via structural compensation of altering metabolic flux through alternative pathways¹⁹; the residual tumor cells will gain even stronger survival ability to escape from immune surveillance after a short period of the “cask effect”^{20,21}. With the advent of next-generation sequencing (NGS) and next-generation of protein profiling, multidimensional diagrams depicting metabolic reprogramming-related alternations in common tumor-associated microenvironment have been created^{22,23}. In addition, recent studies demonstrate inter- and intra-cancer heterogeneity of innate and acquired immune resistance through visualized Figures and tables²⁴. Recent years witnessed the development of immunotherapy with checkpoint inhibitors and other immunotherapies including vaccines and chimeric antigen receptor-T (CAR-T) cells²⁵, highlighting an attractive focus, the interactions between tumor immunity infiltration and “metabolic reprogramming”²⁶. Particularly for survival, the growing tumor must alter immune responses and/or establish a localized microenvironment in response to the immune stress via inhibiting the tumoricidal activity of immune cells^{27,28}. In the tumor-associated microenvironment, regional hypoxia, low pH, loss of collagenase resulting from structural changes in the expression profiles of metabolic enzymes are even accompanied by the dual effect of immunosuppression and/or “cancer immunoediting” that facilitates tumor growth²⁹. There are three phases of this effect, respectively, elimination, balance, and escape³⁰. In the tumor-specific immune microenvironment, the single role of abnormal glucose metabolism network, TCA cycle, glycolysis, and lactose metabolism seemingly assist tumor cells in escaping from the immune surveillance³¹.

Results

I. Differences in glucose metabolism between tumor cells with “metabolic reprogramming” versus normal cells

We performed parallel comparisons of mRNA expression levels of 26 genes encoding metabolic enzymes between 33 common tumor types in the TCGA database and used CPTCA database was for verification. Through comparing between Figure.1A (mRNA expression levels of genes encoding metabolic enzymes in normal cells) and Figure.1B (mRNA expression levels of genes encoding metabolic enzymes in tumor

cells), it can be found that the transformation between anaerobic glycolysis and aerobic oxidation of glucose seemed to be more dependent on phosphoenolpyruvate carboxykinase (PCK/PEPCK) encoded by PCK1/2. Combining with metabolic enzyme protein expression level (Figure.1C), though PCK/PEPCK was not expressed or lowly expressed in most of the samples, it showed significant upregulation in some patients. (The difference in PCK/PEPCK gene expression will be explained in more detail in Figure.3.) Although the expression pattern of PCK1/2 in a variety of tumors is obviously different, it is most obvious in tumors such as PCK1 in BRCA, CHOL, COAD, KICH, KIRC, KIRP, LIHC, READ and PCK2 in CHOL, COAD, KICH, KIRC, KIRP, LIHC. It is not difficult to see from these data that the significant differential expression of PCK/PEPCK is more common in the digestive system and urinary system tumors in daily clinical practice.

As shown in Figure.1, we found an interesting phenomenon that there were tremendous fluctuations in the component percentage of enzyme genes associated with glycolysis in tumor cells. Even after adjustment, there still existed a broad range of differences in some enzyme gene expression between not only distinct clinical stages in the same tumor but also different tumor types. Specifically, the fluctuations of the three enzymes, phosphofructokinase, aldolase, and enolase respectively encoded by PFKM, ALDOC, and ENO1/2 were most prominent, indirectly reflecting a stronger perception and ability of tumor cells in response to energy state disturbance. The cascade amplification of glucose metabolic flux is affected by the blocking effect of PCK/PEPCK, together with the structurally stable expression of GAPDH, phosphoglycerate kinase and phosphoglycerate mutase. In addition, tumor cells also take advantage of the metabolism with the involvement of the encoding genes, FPKM, ALDOC, and GAPDH, in order to mediate the transition between fructose-1, 6-diphosphate, dihydroxyacetone phosphate, and glyceraldehyde 3-phosphate. Tumor cells use this minor cycle in glycolysis as a “water-hammer arrestor” to protect them against sudden changes in the living environment or living stress from antitumor agents targeting glucose metabolic enzymes^{32,33}. Actually, changes in the ATP/AMP ratio can allosterically regulate the expression of key metabolic enzymes³⁴, controlling glucose metabolism ceasing at the glycolysis phase or pushing glucose flowing toward the TCA cycle and the electron transport chain of oxidative phosphorylation. By this means, the outlet of glucose metabolic flux has been changed and thus tumor cells can ultimately survive in different contexts³⁵.

II. Differences between distinct tumor energy metabolic pattern

In Figure.2, dotted caisson diagrams depict the levels of different metabolic enzymes in 18 solid malignant tumours. Groups are sorted according to metabolic enzyme coding genes based on the source of organization, respectively. Due to the data in the CPTAC database, the objective data content and the data that can be used for horizontal comparison only exist in a few tumors originating from the brain, breast, colorectal, lung, ovary, stomach, bladder, kidney, etc. These recorded data are not as rich as the data in TCGA, and there are more vacancies. Therefore, we only use the protein data in the CPTAC database to verify the conclusions of TCGA gene expression data.

III. Relationships between glucose metabolism and “hazard rate” for tumor patients

The selected 26 genes encoding metabolic enzymes, as gene markers, were reversely labeled into 33 tumors from the database to plot hazard ratios of different genes encoding metabolic enzymes for each tumor patient (Figure.3). The overall high expression of metabolic enzyme gene profiles indicated exuberant glucose metabolism in tumor cells. In combination with EMR, the obtained results suggest that the hazard ratios of metabolic enzyme gene profiles depend on the glucose metabolic background of distinct tumors, showing positive association with stemness indices. The analyses of the hazard ratios of 26 enzymes showed that ACO1 ($p < 0.001$; HR = 0.894), ACO2 ($p < 0.001$; HR = 0.923), IDH3G ($p = 0.017$; HR = 0.928), MDH1 ($p < 0.001$; HR = 0.875), PCK ($p < 0.001$; HR = 0.917) and SUCLG1 ($p < 0.001$; HR = 0.838) were negatively associated with hazard ratios (Figure.3B). Instead, the hazard ratios of ALDOA ($p < 0.001$; HR = 1.113), ALDOC ($p < 0.001$; HR = 1.059), ENO1 ($p < 0.001$; HR = 1.262), GAPDH ($p < 0.001$; HR = 1.314), IDH1 ($p < 0.001$; HR = 1.084), IDH3B ($p = 0.007$; HR = 1.093), PFKP ($p < 0.001$; HR = 1.075), PGAM1 ($p < 0.001$; HR = 1.424), PGK1 ($p < 0.001$; HR = 1.258), PKM ($p < 0.001$; HR = 1.186), SDHB ($p < 0.001$; HR = 1.188), SDHD ($p < 0.001$; HR = 1.117) and TPI1 ($p < 0.001$; HR = 1.242) were positively and significantly correlated with survival hazard ratios in patients ($p < 0.05$) (Figure.3B). Based on the hazard ratios, patients were stratified into the high-risk group and the low-risk group. First, a total of 16 metabolic enzymes in the glucose metabolic profiles affecting the prognosis of patients were assessed (Figure.4A). Figure.4B showed the hazard ratios for the survival distribution of each patient. With a mortality rate of 55.15%, the high-risk group was at a higher risk of death. The mortality of the low-risk group was 37.13%. The Chi-square test presented a significant difference in mortality between the two groups ($p < 0.05$). ROC curves were plotted, and the mean AUC was 0.683 ($P < 0.05$) (Figure.4C). Besides, we employed ROC curve analysis to compare survival prediction values based on mRNA expression traits of all glucose metabolic enzyme profiles. The results showed that LDHA (AUC = 0.603), PGAM1 (AUC = 0.598) and GAPDH (AUC = 0.591) had greater survival prediction value. Moreover, after we excluded enzymes with low survival prediction values and only retained those with an AUC > 0.5, the mean AUC of ROC curves was 0.73 ($P < 0.01$) (Figure.4C).

IV. Associations between glucose metabolism, immune subtypes, and immune cell infiltration

The analysis of immune subtypes demonstrated that in six different subtypes C1-6 (C1: wound healing, C2: IFN- γ dominant, C3: inflammatory, C4: lymphocyte depleted, C5: immunologically quiet, and C6: TGF- β dominant)^{36,37}, there existed strong associations between all of the 26 enzyme-encoding genes in the pan-cancer glucose metabolic pathways and immune subtypes (Figure.5, $p < 0.001$). The overexpression of ACO2, ALDOC, ENO2 and PFKP, together with the down-regulation of LDHA, PCK2, PGK1 and TPI1 was tightly associated with C5 (immunologically quiet, manifested by the lowest lymphocyte level, increased macrophage reactions, and the predominance of M2 macrophages), indicating that the expression levels of the eight enzyme-encoding genes were related to immune escape. This trait indicates that the tumor

immune subtypes can be altered via inhibiting or overexpressing the mentioned glucose metabolic enzymes. Concerning this phenomenon, we comprehensively analyzed the proportions of distinct immune cells in the cancer immune microenvironment. As indicated from Figure.6, the effector cells that mediated the acquired immunity, including plasma cells ($p < 0.01$), resting natural killer (NK) cells ($p < 0.01$), monocytes ($p < 0.01$), M2 macrophages ($p < 0.01$), activated mast cells ($p < 0.01$), and neutrophils ($p < 0.01$), showed low proportions. By contrast, T follicular helper cells ($p < 0.01$), T regulatory cells (Tregs) ($p < 0.01$), activated natural killer (NK) cells ($p = 0.025$), M0 macrophages ($p < 0.01$), resting dendritic cells ($p = 0.012$), resting mast cells ($p < 0.01$) that mediated the congenital immunity, exhibited a significantly weaker killing effect on tumor cells than those that mediated the humoral and cellular immune responses, regardless of their high expression levels.

V.EMR and Tumor-Associated Immune Cells

Due to the pattern of immune cells infiltrating in different tumor microenvironments is too complicated, in order to combine with our main research field, we only use tumors originating in the liver to explain

1. The low-expression of GAPDH (Figure.7H, $p < 0.05$), IDH2 (Figure.7J, $p < 0.05$), IDH3B (Figure.7K, $p < 0.05$), and PGK1 (Figure.7T, $p < 0.001$) and the high-expression of IDH3G (Figure.7L, $p < 0.05$) and MDH1 (Figure.7N, $p < 0.001$) inhibited the activity of B cells. LDHA (Figure.7M, $p < 0.05$) overexpression stimulated the activity of B cells. Obviously, either SDHB (Figure.7W, $p < 0.01$) down-expression or overexpression could inhibit B cell activity.
2. T cells are the key participants in the host immune system to respond to tumor cells. These cells were comprehensively analyzed in this study, and it was found that, on the one hand, the low expression levels of ENO2 (Figure.7F, $p < 0.05$), GAPDH (Figure.7H, $p < 0.01$), PFKP (Figure.7R, $p < 0.01$), PGK1 (Figure.7T, $p < 0.05$) and TPI1 (Figure.7Z, $p < 0.05$), whereas the high expression levels of FH (Figure.7G, $p < 0.05$) suppressed the activity of CD8 + T cells; in addition, the low expression of PGAM1 (Figure.7S, $p < 0.05$) stimulated the activity of CD8 + T cells. On the other hand, the over-expression of ALDOC (Figure.7D, $p < 0.001$), IDH1 (Figure.7I, $p < 0.05$), PKM (Figure.7U, $p < 0.001$) and SDHA (Figure.7V, $p < 0.01$) suppressed the activity of CD4 + T cells. Undeniably, once the differentiated effector T cells, like CD4 + or CD8 + T cells are activated, they will raise the demands for bioenergy and biosynthesis to satisfy the subsequent differentiation and rapid proliferation³⁸. The low-expression of MDH1 (Figure.7N, $p < 0.001$), PFKP (Figure.7R, $p < 0.001$), and PGK1 (Figure.7T, $p < 0.05$) alongside the high-expression of ALDOA (Figure.7C, $p < 0.001$), ALDOC (Figure.7D, $p < 0.05$), IDH3G (Figure.7L, $p < 0.001$), and PCK1 (Figure.7O, $p < 0.05$) inhibited the activity of macrophages. The low-expression of PCK2 (Figure.7P, $p < 0.05$) and PGAM1 (Figure.7S, $p < 0.05$) could stimulate macrophage activity. Tumor-associated macrophages (TAMs) is immunosuppressive M2 macrophages, which are abundant in the tumor microenvironment.
3. Macrophages (predominantly glycolysis in M1 macrophages) can promote hereditary changes and cancer-related inflammation through the generation of RNI, ROI, and inflammatory cytokines (e.g., TNF, IL-1, and IL-6), resulting in the occurrence of tumors³⁹. Additionally, M2 macrophages (mainly oxidative phosphorylation) facilitate immunosuppression, extracellular matrix remodeling, the

spillover of tumor cells⁴⁰, and metastases of metastasized tumors through the generation of anti-inflammatory cytokines (IL-10 and TGF- β), cathepsins, and metalloproteinases (MMPs)^{41,42}.

4. Tumor-associated neutrophils (TANs) may have both protumor and antitumor properties⁴³. When lacking tumor-derived TGF- β , TANs promote CD8 + T cell responses and its antitumor activity. In the presence of TGF- β , TANs have protumor activity^{44,45}. The low-expression of ENO1 (Figure.7E, $p < 0.05$) and SDHA (Figure.7V, $p < 0.01$) alongside the high-expression of FH (Figure.7G, $p < 0.05$), IDH3G (Figure.7L, $p < 0.01$), PCK1 (Figure.7O, $p < 0.01$), PGAM1 (Figure.7S, $p < 0.001$), and PGK1 (Figure.7T, $p < 0.001$) inhibited neutrophil activity. The low-expression of PGAM1 (Figure.7S, $p < 0.01$) stimulated neutrophil activity.
5. Dendritic cells (DCs) are professional antigen-presenting cells bridging innate immunity and adaptive immunity⁴⁶. The low-expression of GAPDH (Figure.7H, $p < 0.05$), IDH1 (Figure.7I, $p < 0.01$), IDH2 (Figure.7J, $p < 0.05$), PGK1 (Figure.7T, $p < 0.001$), and SDHB (Figure.7W, $p < 0.001$) as well as IDH3G high-expression suppressed dendritic cell activity. The low-expression of PCK2 (Figure.7P, $p < 0.05$) and PGAM1 (Figure.7S, $p < 0.05$) could stimulate dendritic cell activity.
6. In addition, not all metabolic enzymes affect immune cells in the tumor-related microenvironment. In Figure.7, we can find that (A)ACO1, (B)ACO2, (M) LDHA, (Q)PFKM, and (X)SDHD, (Y)SUCLG1 have very weak effects on these six main kinds of immune cells. Because of the enzymes Aconitase (ACO) and Lactate Dehydrogenase (LDHA) encoded by these genes mainly enzymatically catalyze one-way reactions. Alternatively, Phosphoglycerate Mutase (PFKM), Succinate Dehydrogenase (SDH) and Succinyl-Coenzyme A (SUCLG) catalyze the weakened alternative glucose pathway.

Discussion

Although the theory of “Warburg effect” claims: under aerobic conditions, there is a phenomenon of increased glucose uptake and the transform of glucose into lactic acids⁴⁷, and cancer characteristics somewhat rely on the regulation of multiple transcriptional regulation factors in the nucleus, including HIF-1 α/β , STAT3, and β -catenin^{6,48,49}. We therefore mapped the global glucose metabolic network, Figure.8 presents the expression levels of proteins encoded by various enzyme genes in Figure.1, showing that phosphoenolpyruvate, pyruvate, and oxaloacetic acid are the three important factors directing the glucose metabolic flux in tumor cells. Pyruvate kinase and the pyruvate dehydrogenase complex are the central links of pyruvate metabolism, catalyzing the oxidative decarboxylation of pyruvic acid to Ac-CoA and transforming NAD⁺ to NADH in the mitochondria⁵⁰. The key enzymes involved in the two glycolysis types are regulated by the PDH kinase (PDK), Ac-CoA levels, nutrient levels, the NAD⁺/NADH ratio, and the intracellular oxygen concentration, which together decide whether the glucose flows to the TCA cycle in the mitochondria^{51–53}. Besides glycolysis, there exists a reverse cycle, gluconeogenesis, in normal cells. By contrast, the plummet of PCK/PEPCK expression (Figure.1) in tumor cells indirectly indicates that there only can be very slight gluconeogenesis in tumor cells. Different from normal cells, the metabolic input of pyruvate by glycolysis into the TCA cycle in tumor cells ultimately generates little chance of obtaining phosphoenolpyruvate via the reverse cycle⁵⁴. The structurally stable expression of TCA-cycle

related enzymes functions as a circling gyroscope to automatically counterbalance the unstable factors in the microenvironment. Moreover, the TCA cycle still receives Ac-CoA supported by fatty acid metabolism, glutamine, and the anaplerotic flux of multiple amino acids (Figure.8)⁶. One aim is to synthesize nonessential amino acids to balance the biomass supply in tumor cells. Additionally, it aims to offer reducing equivalents to enter the reducing equivalent pool produced in the process of the metabolism of sugar, fat, and protein, promoting glucose into the electron transport chain for oxidative phosphorylation in the mitochondria ultimately. In this way, the mitochondrial functions in tumor cells can be secured to provide a large amount of ATP for cell survival^{55,56}.

Up to the present, although researchers are extremely familiar with the basic knowledge frame of glucose metabolism and there are voluminous studies of related metabolic enzymes and their encoding genes⁷, the more intricate metabolic networks perplex the identification of key targets optimal for interventions⁸. Relative studies often concentrate on a single enzyme or the nearby upstream or downstream pathways to investigate changes in the metabolic flux and speculate possible alternations in metabolic networks as a whole by measuring expression changes in metabolic substrates or products⁹. Although these studies have demonstrated the regulatory mechanisms of controlling glucose metabolism in various proliferative and non-proliferative cells via revealing changes in metabolic demands¹⁰, gain-of-function mutations in tumor cells, and structural alternations, such as mutations of regulatory elements of genes in the receptor promoter¹¹, alternative splicing of encoding genes^{12,13}, and isozyme replacement¹⁴, can help glucose metabolism out of dependence on growth factors physiologically¹⁵. Recent studies demonstrated the fact that the single control of some links in the glucose metabolism in tumor cells, including knockdown of mitochondrial pyruvate carrier (MPC)¹⁶, knockdown of the tricarboxylic acid (TCA)-cycle enzymes to reduce the activity¹⁷, or a shift in PKM2 to PKM1 by alternative splicing⁶, can obtain satisfactory outcomes in in vitro experiments with interventions¹⁸. However, in real patients, tumor cells obtain nutrients and restore metabolism already being inhibited via structural compensation of altering metabolic flux through alternative pathways¹⁹; the residual tumor cells will gain even stronger survival ability to escape from immune surveillance after a short period of the “cask effect”^{20,21}. With the advent of next-generation sequencing and next-generation of protein profiling, multidimensional diagrams depicting immune-related alternations in common cancer genome have been created^{22,23}. In addition, they demonstrate inter- and intra-cancer heterogeneity of innate and acquired immune resistance through visualized figures and tables²⁴. Recent years witnessed the development of immunotherapy with checkpoint inhibitors and other immunotherapies including vaccines and chimeric antigen receptor-T (CAR-T) cells²⁵, highlighting an attractive focus, the interactions between tumor immunity process and “metabolic reprogramming”²⁶. Particularly for survival, the growing tumor must alter immune responses and/or establish a localized microenvironment in response to the immune stress via inhibiting the tumoricidal activity of immune cells^{27,28}. In the microenvironment, regional hypoxia, low pH, loss of collagenase resulting from structural changes in the expression profiles of metabolic enzymes are even accompanied by the dual effect of immunosuppression and/or “cancer immunoediting” that facilitates tumor growth²⁹. There are three phases of this effect, respectively, elimination, balance, and escape³⁰. In

the tumor-specific immune microenvironment, the single role of abnormal glucose metabolism network, TCA cycle, glycolysis, and lactose metabolism seemingly assist tumor cells in escaping from the immune surveillance^{31,57,58}. In addition, they can also alter the subtypes of the immune microenvironment where tumor cells reside and the count of immunologic effector cells decreases at the same time, make most antigen-presenting cells to be activated, and inhibit the activity of cytotoxic T cells⁵⁹. Tumor immune surveillance can ensure the majority of malignant cells to be eliminated (or controlled) at the early stage by the immune system^{60,61}. Malignant transformation allows tumor cells to gradually obtain the ability to escape from “adaptive immunity”, which is accompanied by glucose metabolic reprogramming, adaptive reassortment, and changes in the immune microenvironment⁶². A tumor is the main reason accounting for the dynamic unbalance of the homeostasis of tissues of origin, breaking the intrinsic metabolic patterns, and creating a new environment for the benefit of tumor cell metabolism⁶³. The tumor microenvironment (TME) erodes the metabolism and function of the matrix, which also facilitates immune cell infiltration at the early stage. Aerobic glycolysis under the “Warburg effect” usually supports the immortal cell proliferation in cancers, and serves as the identical metabolic pathway that promotes the optimal effector function in immune cells^{31,64}.

Previous studies showed that multiple immune effector cells might share similar metabolic pathways with tumor cells in the TME⁶⁵. Figure.9 showed the associations between glucose metabolism, immune subtypes, and immune cell infiltration. Interestingly, the process of immune cell activation is accompanied by the “adaptive reassortment of glucose metabolism”, and the distinctive “metabolic adaptive reassortment” in immune cells is regarded as a critical trait of immune cell activation by a large number of researchers^{63,66,67}. Subpopulations of immune cells with high metabolic activity can lead to regional nutrient consumption, hypoxia, acidity, and metabolite accumulation in the TME, finally resulting in the establishment of metabolic competition between cancer cells and immune cells^{68,69}. Physiologically, immune surveillance ensures that immune cells can fast initiate an immune mechanism to eradicate “bad cells” after they recognize these alien cells to safeguard the internal environment⁷⁰. However, tumor cells can complete the evasion of immune surveillance in the established tumor immunosuppressive environment (TIME)^{71,72}. The analysis of immune subtypes demonstrated that in six different subtypes C1-6 (C1: wound healing, C2: IFN-g dominant, C3: inflammatory, C4: lymphocyte depleted, C5: immunologically quiet, and C6: TGF- β dominant)^{36,37}, there existed strong associations between all of the 26 enzyme-encoding genes in the pan-cancer glucose metabolic pathways and immune subtypes (Fig. 8, $p < 0.001$). The overexpression of ACO2, ALDOC, ENO2 and PFKP, together with the down-regulation of LDHA, PCK2, PGK1 and TP11 was tightly associated with C5 (immunologically quiet, manifested by the lowest lymphocyte level, increased macrophage reactions, and the predominance of M2 macrophages), indicating that the expression levels of the eight enzyme-encoding genes were related to immune escape. This trait indicates that the tumor immune subtypes can be altered via inhibiting or overexpressing the mentioned glucose metabolic enzymes. Concerning this phenomenon, we comprehensively analyzed the proportions of distinct immune cells in the pan-cancer immune microenvironment. As supported by the metabolic enzyme gene profile analysis and immune cell sorting,

immune subtypes, agents and molecular targets, we believe that whatever tissue the tumor is derived from, it exhibits characteristic metabolic patterns and immune subtypes. Tumor cells inhibit functions of immune cells via the metabolism of themselves. Tumor cells gain energy from glucose through aerobic glycolysis and glutaminolysis, depleting glucose and L-glutamine in the tumor microenvironment and producing lactic acids^{73–75}. This process leads to low pH in the tumor microenvironment, thus suppressing the activity of T cells and NK cells and facilitating Treg cell differentiation, MDSC amplification, and M2 macrophage polarization⁷⁰. Tumor therapy decisions can be made based on metabolomics and immunosorting analysis. Under such frame, precisely blocking the specific metabolic pathways in patients in combination with agents activating specific immune cells can effectively prolong the survival of patients with ameliorated prognosis.

Conclusions

In the present study, we explored the general metabolic requirements of glucose metabolism in cancer cells and described cellular metabolic pattern landscapes of tumor immune infiltration. We aimed to elucidate structural alternations in the metabolic flux of cancer cells and associations between the infiltration by various types of B cells, T cells, and macrophages, and their subtypes in various different immune subtypes and clinical application⁷⁶. Meanwhile, with hepatocellular carcinoma (HCC) as an example, we investigated relationships between glucose metabolic enzymes and six major immune cells. In summary, metabolic enzymes are critical in glucose metabolism, regulating energy metabolism reprogramming (EMR) and adaptive mitochondrial reprogramming (AMR) in tumor cells^{6,77}. These affect “cancer immunoediting” that exerts dual effects³⁰, and they jointly play significant roles in tumor occurrence⁷⁸, development, invasion and metastasis, immune responses, as well as the diagnosis, treatment and prognosis for tumor patients. Finally, it is believed that with in-depth studies of metabolomics and immune mechanism for tumor cells, researchers will obtain a deeper understanding of interactions between intricate metabolic networks and immune responses. Moreover, the current review may help inform cancer metabolic-immuno-therapy and facilitate the development of precision metabolic-immuno-oncology.

Materials & Methods

Data Acquisition and Collection

The supporting data, processed data and clinical data can be found at the legacy archive of the GDC (<https://portal.gdc.cancer.gov/legacy-archive/search/f>) and the Pan-cancer Atlas publication page (<https://gdc.cancer.gov/about-data/publications/pancanatlas>). RTCGA Toolbox package (version 3.6) in R (version 4.0.1) provided the data of pan-cancer cases and RNA-seq expression outcomes. Additionally, the present study achieved the expression data of metabolic enzyme coding genes from The Cancer Genome Atlas (TCGA: <https://portal.gdc.cancer.gov>) & UCSC Genome Browser Home (<https://genome.ucsc.edu>) and proteomic data from CPTAC (<https://cptac-data-portal.georgetown.edu>) in

terms of pan-cancer^{79,80}. The sources of tumor tissue cover stomach, pancreas, liver, esophagus, colon, bile duct and so on. In addition, we also employed single sample gene set enrichment analysis (ssGSEA) (GSEA software 3.2)⁸¹ to identify immune cell types that are over-represented in the tumor microenvironment. Finally, a deconvolution approach was applied using the tool CIBERSORT and a custom model to modify RNA-sequencing data from TCGA & UCSC and proteomic data from CPTAC to be used as input of the deconvolution algorithm⁸². In the mentioned databases in March 2021, the current review obtained the data employed here.

Statistical Analyses

SPSS software 23.0 (IBM Corporation, Armonk, NY, USA) was employed for data analyzing. Based on TCGA and UCSC Pan-Cancer dataset, this study adopted R/Bioconductor package of edgeR⁸³ for determining miRNAs with differential expression. All thresholds were set at the absolute $\log_2(\text{count} + 1)$ fold change and the false discovery rate (FDR) < 0.05. Boxplots were adopted in terms of discrete variables for the measurement of diversifications in expression, and influences exerted by Biological characteristics on metabolic enzyme coding genes expression were studied by Kolmogorov-Smirnov test (K-S test)⁸⁴. The current work presented alterations in expression between respective group by scatter plots. GraphPad Prism 7.0 software (GraphPad Software, Inc.) was employed to analyze the differentially expressed condition of metabolic enzyme coding genes in a range of tumor tissues. Scatter plots and histograms were adopted for discrete parameters in order to measure diversifications in expression between a range of tissues. Additionally, influences exerted by tumor tissue of origin on metabolic enzyme coding genes expression were analyzed using the mean \pm SD. Receiver-operating characteristic curve (ROC) was plotted by “p-ROC package” (version 1.0.7) for evaluating the diagnosing ability. We divide cases to groups with high and low metabolic enzyme coding genes expression by the best cutoff value of OS determined by the Youden index⁸⁵. Correlation coefficient analyses were performed using R software. A correlation coefficient $R > 0.5$ was considered for indicating a strong correlation. Cox analysis was employed on the effect exerted by metabolic enzyme coding genes expression on the overall survival and relapse-free survival of cases⁸⁶. Kaplan–Meier curves were adopted for the comparison of the diversifications in the overall survival and relapse-free survival using survival package in R⁸⁷. Log rank tests (corresponding to a two-sided z test) were used to compare overall survival between patients in different groups, and hazard ratio (HR) (95% confidence interval) was provided for comparison of two groups. The p-values were adjusted for multiple testing based on the false discovery rate (FDR) using the Benjamini-Hochberg method. Patients for each cancer were divided in two groups based on median immunephenoscore. Cox regression analyses were performed and illustrated as forest plot showing $\log_2(\text{HR})$ and 95% confidence interval and tested the proportional hazard assumptions.

Immune Cellular Fraction Estimates

The relative fraction of 22 immune cell types within the leukocyte compartment were estimated using CIBERSORT⁸⁸, applying CIBERSORT to TCGA & UCSC and CPTAC data. CIBERSORT (cell-type identification

by estimating relative subsets of RNA transcripts)⁸⁹ uses a set of 22 immune cell reference profiles to derive a base (signature) matrix which can be applied to mixed samples to determine relative proportions of immune cells⁹⁰. Several key immune genes in the signatures cluster can be used to classify and analyze the subtypes of immune infiltration(C1-C6)⁹¹.

Correlation Between Metabolic Enzymes and Immune Infiltrating Cells

A retrospective dataset of patients with LIHC-cancer from TCGA & UCSC and proteomic data from CPTAC database was analysed for the infiltration levels of six types of immune cells using Tumor IMmune Estimation Resource (TIMER) (<https://cistrome.shinyapps.io/timer/>)⁹². The RNA sequencing data was applied to select metabonomics features to build the metabolic enzymes signatures for extrapolating the infiltration levels of immune cells in the training cohort. The developed metabolic enzymes were examined in the testing cohort based on Pearson’s correlation. In addition, we used software CellMiner (<https://discover.nci.nih.gov/cellminer/home.do>)⁹³ to screen and analyze drugs in metabolic enzyme related homicide cases.

Abbreviations

TCGA and UCSC Tumor Type

ACC	Adrenocortical carcinoma
BLCA	Bladder Urothelial Carcinoma
BRCA	Breast invasive carcinoma
CESC	Cervical squamous cell carcinoma and endocervical adenocarcinoma
CHOL	Cholangiocarcinoma
COAD	Colon adenocarcinoma
READ	Rectum adenocarcinoma Esophageal carcinoma
DLBC	Lymphoid Neoplasm Diffuse Large B-cell Lymphoma
ESCA	Esophageal carcinoma
GBM	Glioblastoma multiforme
HNSC	Head and Neck squamous cell carcinoma
KICH	Kidney Chromophobe
KIRC	Kidney renal clear cell carcinoma

KIRP	Kidney renal papillary cell carcinoma
LAML	Acute Myeloid Leukemia
LGG	Brain Lower Grade Glioma
LIHC	Liver hepatocellular carcinoma
LUAD	Lung adenocarcinoma
LUSC	Lung squamous cell carcinoma
MESO	Mesothelioma
OV	Ovarian serous cystadenocarcinoma
PAAD	Pancreatic adenocarcinoma
PCPG	Pheochromocytoma and Paraganglioma
PRAD	Prostate adenocarcinoma
READ	Rectum adenocarcinoma
SARC	Sarcoma
SKCM	Skin Cutaneous Melanoma
STAD	Stomach adenocarcinoma
STES	Stomach and Esophageal carcinoma
TGCT	Testicular Germ Cell Tumors
THCA	Thyroid carcinoma
THYM	Thymoma
UCEC	Uterine Corpus Endometrial Carcinoma
UCS	Uterine Carcinosarcoma
UVM	Uveal Melanoma

Glucose Metabolizing Enzymes

AOC Aconitase

ALDOA Aldolase A

ENO Enolase

FH Fumarate Hydratase

GAPDH Glyceraldehyde-3-phosphate Dehydrogenase

IDH Isocitrate Dehydrogenase

LDHA Lactate Dehydrogenase

MDH Malate Dehydrogenase

PCK/PEPCK Phosphoenolpyruvate Carboxy-kinase

PFKM Phosphoglycerate Mutase

PFKP Phosphofructokinase

PKM Pyruvate Kinase M

PGK Phosphoglycerate Kinase

SDH Succinate Dehydrogenase

SUCLG Succinyl-Coenzyme A

TPI Triose Phosphate Isomerase

Others

Immune Subtypes

C1 Wound Healing

C2 IFN-g Dominant

C3 Inflammatory

C4 Lymphocyte Depleted

C5 Immunologically Quiet

C6 TGF- β Dominant

AA Amino Acid Residues

Ac-CoA Acetyl Coenzyme-A

AMR Adaptive Mitochondrial Reprogramming

ATP Adenosine Triphosphate

CAR-T Chimeric Antigen Receptor-T

Cox Proportional Hazards Model

EMT Epithelial–Mesenchymal Transition

EMR Energy Metabolism Reprogramming

FADH2 Flavine Adenine Dinucleotide

FDR False Discovery Rate

GSEA Gene Set Enrichment Analysis

HIF-1 α Hypoxia Inducible Factor-1 α

HIF-1 β Hypoxia Inducible Factor-1 β

HCC Hepatocellular Carcinoma

CTLA-4 Cytotoxic T-Lymphocyte-Associated Protein 4

LDH Lactate Dehydrogenase

PD-1 Programmed Cell Death Protein 1

pH Hydrogen Ion Concentration

PKM1 M1 Isoform of Pyruvate Kinase

PKM2 M2 Isoform of Pyruvate Kinase

MPC Mitochondrial pyruvate carrier

MiR/miRNA MicroRNA

MMP Metalloproteinases

NADH	Nicotinamide Adenine Dinucleotide
NGS	Next-generation Sequencing
OS	Overall Survival
ROC	Receiver Operating Characteristic Curve
TAM	Tumor-associated Macrophages
TAN	Tumor-associated Neutrophils
TCA	Tricarboxylic Acid Cycle
TCGA	The Cancer Genome Atlas
TCR	T Cell Receptor
TIME	Tumor Immunosuppressive Environment
TIMER	Tumor IMMune Estimation Resource
TME	Tumor Microenvironment
Treg	Regulatory T Cell

Declarations

Ethics approval and consent to participate

Not applicable.

Consent for publication

Not applicable.

Competing interests

The authors declare that they have no competing interests.

Funding

This study was supported by the Key Science and Technology R&D Project of Jilin Science and Technology Department, No.20180201055YY. (Sponsor: Zihui Meng)

Authors' contributions

ZZ and Meng ZH conceived of the presented idea. ZZ and Zhang XW developed the theory and performed the computations. ZZ, Zhang XW and Lin Nan verified the analytical methods. Meng ZH encouraged ZZ and Zhang XW to conduct experimental research, organize experimental data into manuscripts and supervised the findings of this work. All authors commented on drafts and approved the final version. All authors participated in the decision to submit for publication.

Acknowledgments

We were grateful to Prof. Meng ZH for his sponsorship to this project. And Dr. Qu Kuo's and Deng Xinyue's spiritual support for our team.

Availability of data and material

Data acquisition and processing methods have been described in the part of Materials and Methods.

References

1. Vander Heiden, M. G., Cantley, L. C. & Thompson, C. B. Understanding the Warburg effect: the metabolic requirements of cell proliferation. *Science*. **324**, 1029–1033 <https://doi.org/10.1126/science.1160809> (2009).
2. Cairns, R. A., Harris, I. S. & Mak, T. W. Regulation of cancer cell metabolism. *Nat Rev Cancer*. **11**, 85–95 <https://doi.org/10.1038/nrc2981> (2011).
3. Liberti, M. V. & Locasale, J. W. The Warburg Effect: How Does it Benefit Cancer Cells? *Trends Biochem Sci*. **41**, 211–218 <https://doi.org/10.1016/j.tibs.2015.12.001> (2016).
4. Jang, C., Chen, L. & Rabinowitz, J. D. Metabolomics and Isotope Tracing. *Cell*. **173**, 822–837 <https://doi.org/10.1016/j.cell.2018.03.055> (2018).
5. Wishart, D. S. Metabolomics for Investigating Physiological and Pathophysiological Processes. *Physiol Rev*. **99**, 1819–1875 <https://doi.org/10.1152/physrev.00035.2018> (2019).
6. Zhang, Z. *et al.* PKM2, function and expression and regulation. *Cell Biosci*. **9**, 52 <https://doi.org/10.1186/s13578-019-0317-8> (2019).
7. DeBerardinis, R. J. & Chandel, N. S. Fundamentals of cancer metabolism. *Sci Adv*. **2**, e1600200 <https://doi.org/10.1126/sciadv.1600200> (2016).
8. Dai, Z., Ramesh, V. & Locasale, J. W. The evolving metabolic landscape of chromatin biology and epigenetics. *Nat Rev Genet*. <https://doi.org/10.1038/s41576-020-0270-8> (2020).
9. Saxton, R. A. & Sabatini, D. M. mTOR Signaling in Growth, Metabolism, and Disease. *Cell*. **168**, 960–976 <https://doi.org/10.1016/j.cell.2017.02.004> (2017).
10. Berndt, N. & Holzhutter, H. G. Mathematical Modeling of Cellular Metabolism. *Recent Results Cancer Res*. **207**, 221–232 https://doi.org/10.1007/978-3-319-42118-6_10 (2016).
11. Brennan, C. W. *et al.* The somatic genomic landscape of glioblastoma. *Cell*. **155**, 462–477 <https://doi.org/10.1016/j.cell.2013.09.034> (2013).

12. Sveen, A., Kilpinen, S., Ruusulehto, A., Lothe, R. A. & Skotheim, R. I. Aberrant RNA splicing in cancer; expression changes and driver mutations of splicing factor genes. *Oncogene*. **35**, 2413–2427 <https://doi.org/10.1038/onc.2015.318> (2016).
13. Kedzierska, H. & Piekietko-Witkowska, A. Splicing factors of SR and hnRNP families as regulators of apoptosis in cancer. *Cancer Lett*. **396**, 53–65 <https://doi.org/10.1016/j.canlet.2017.03.013> (2017).
14. Dayton, T. L., Jacks, T. & Vander Heiden, M. G. PKM2, cancer metabolism, and the road ahead. *EMBO Rep*. **17**, 1721–1730 <https://doi.org/10.15252/embr.201643300> (2016).
15. Vander Heiden, M. G. & DeBerardinis, R. J. Understanding the Intersections between Metabolism and Cancer Biology. *Cell*. **168**, 657–669 <https://doi.org/10.1016/j.cell.2016.12.039> (2017).
16. Caruso, P. *et al.* Identification of MicroRNA-124 as a Major Regulator of Enhanced Endothelial Cell Glycolysis in Pulmonary Arterial Hypertension via PTBP1 (Polypyrimidine Tract Binding Protein) and Pyruvate Kinase M2. *Circulation*. **136**, 2451–2467 <https://doi.org/10.1161/CIRCULATIONAHA.117.028034> (2017).
17. Son, J. *et al.* Glutamine supports pancreatic cancer growth through a KRAS-regulated metabolic pathway. *Nature*. **496**, 101–105 <https://doi.org/10.1038/nature12040> (2013).
18. Danhier, P. *et al.* Cancer metabolism in space and time: Beyond the Warburg effect. *Biochim Biophys Acta Bioenerg*. **1858**, 556–572 <https://doi.org/10.1016/j.bbabi.2017.02.001> (2017).
19. Hui, S. *et al.* Glucose feeds the TCA cycle via circulating lactate. *Nature*. **551**, 115–118 <https://doi.org/10.1038/nature24057> (2017).
20. Maynard, A. *et al.* Therapy-Induced Evolution of Human Lung Cancer Revealed by Single-Cell RNA Sequencing. *Cell* **182**, 1232–1251 e1222, doi:10.1016/j.cell.2020.07.017 (2020).
21. Biehs, B. *et al.* A cell identity switch allows residual BCC to survive Hedgehog pathway inhibition. *Nature*. **562**, 429–433 <https://doi.org/10.1038/s41586-018-0596-y> (2018).
22. Huang, X. *et al.* Systematic profiling of alternative splicing events and splicing factors in left- and right-sided colon cancer. *Aging (Albany NY)*. **11**, 8270–8293 <https://doi.org/10.18632/aging.102319> (2019).
23. Toffalori, C. *et al.* Immune signature drives leukemia escape and relapse after hematopoietic cell transplantation. *Nat Med*. **25**, 603–611 <https://doi.org/10.1038/s41591-019-0400-z> (2019).
24. Gajewski, T. F., Schreiber, H. & Fu, Y. X. Innate and adaptive immune cells in the tumor microenvironment. *Nat Immunol*. **14**, 1014–1022 <https://doi.org/10.1038/ni.2703> (2013).
25. June, C. H., O'Connor, R. S., Kawalekar, O. U., Ghassemi, S. & Milone, M. C. CAR T cell immunotherapy for human cancer. *Science*. **359**, 1361–1365 <https://doi.org/10.1126/science.aar6711> (2018).
26. Patel, C. H., Leone, R. D., Horton, M. R. & Powell, J. D. Targeting metabolism to regulate immune responses in autoimmunity and cancer. *Nat Rev Drug Discov*. **18**, 669–688 <https://doi.org/10.1038/s41573-019-0032-5> (2019).
27. Mulder, W. J. M., Ochando, J., Joosten, L. A. B., Fayad, Z. A. & Netea, M. G. Therapeutic targeting of trained immunity. *Nat Rev Drug Discov*. **18**, 553–566 <https://doi.org/10.1038/s41573-019-0025-4>

(2019).

28. Natoli, G. & Ostuni, R. Adaptation and memory in immune responses. *Nat Immunol.* **20**, 783–792 <https://doi.org/10.1038/s41590-019-0399-9> (2019).
29. Jerby-Arnon, L. *et al.* A Cancer Cell Program Promotes T Cell Exclusion and Resistance to Checkpoint Blockade. *Cell* **175**, 984–997 e924, doi:10.1016/j.cell.2018.09.006 (2018).
30. Schreiber, R. D., Old, L. J. & Smyth, M. J. Cancer immunoediting: integrating immunity's roles in cancer suppression and promotion. *Science.* **331**, 1565–1570 <https://doi.org/10.1126/science.1203486> (2011).
31. Riera-Domingo, C. *et al.* Immunity, Hypoxia, and Metabolism-the Menage a Trois of Cancer: Implications for Immunotherapy. *Physiol Rev.* **100**, 1–102 <https://doi.org/10.1152/physrev.00018.2019> (2020).
32. Galluzzi, L., Yamazaki, T. & Kroemer, G. Linking cellular stress responses to systemic homeostasis. *Nat Rev Mol Cell Biol.* **19**, 731–745 <https://doi.org/10.1038/s41580-018-0068-0> (2018).
33. Nakazawa, M. S., Keith, B. & Simon, M. C. Oxygen availability and metabolic adaptations. *Nat Rev Cancer.* **16**, 663–673 <https://doi.org/10.1038/nrc.2016.84> (2016).
34. Han, X. *et al.* Cyclic AMP Inhibits the Activity and Promotes the Acetylation of Acetyl-CoA Synthetase through Competitive Binding to the ATP/AMP Pocket. *J Biol Chem.* **292**, 1374–1384 <https://doi.org/10.1074/jbc.M116.753640> (2017).
35. Joshi, S. *et al.* Adapting to stress - chaperome networks in cancer. *Nat Rev Cancer.* **18**, 562–575 <https://doi.org/10.1038/s41568-018-0020-9> (2018).
36. Li, B., Cui, Y., Nambiar, D. K., Sunwoo, J. B. & Li, R. The Immune Subtypes and Landscape of Squamous Cell Carcinoma. *Clin Cancer Res.* **25**, 3528–3537 <https://doi.org/10.1158/1078-0432.CCR-18-4085> (2019).
37. Shen, R. *et al.* Identification of Distinct Immune Subtypes in Colorectal Cancer Based on the Stromal Compartment. *Front Oncol.* **9**, 1497 <https://doi.org/10.3389/fonc.2019.01497> (2019).
38. MacIver, N. J., Michalek, R. D. & Rathmell, J. C. Metabolic regulation of T lymphocytes. *Annu Rev Immunol.* **31**, 259–283 <https://doi.org/10.1146/annurev-immunol-032712-095956> (2013).
39. Netea-Maier, R. T., Smit, J. W. A. & Netea, M. G. Metabolic changes in tumor cells and tumor-associated macrophages: A mutual relationship. *Cancer Lett.* **413**, 102–109 <https://doi.org/10.1016/j.canlet.2017.10.037> (2018).
40. Na, Y. R., Je, S. & Seok, S. H. Metabolic features of macrophages in inflammatory diseases and cancer. *Cancer Lett.* **413**, 46–58 <https://doi.org/10.1016/j.canlet.2017.10.044> (2018).
41. Xia, Y. *et al.* Engineering Macrophages for Cancer Immunotherapy and Drug Delivery. *Adv Mater.* **32**, e2002054 <https://doi.org/10.1002/adma.202002054> (2020).
42. Italiani, P. & Boraschi, D. From Monocytes to M1/M2 Macrophages: Phenotypical vs. Functional Differentiation. *Front Immunol.* **5**, 514 <https://doi.org/10.3389/fimmu.2014.00514> (2014).

43. Shaul, M. E. & Fridlender, Z. G. Tumour-associated neutrophils in patients with cancer. *Nat Rev Clin Oncol.* **16**, 601–620 <https://doi.org/10.1038/s41571-019-0222-4> (2019).
44. Schernberg, A., Blanchard, P., Chargari, C. & Deutsch, E. Neutrophils, a candidate biomarker and target for radiation therapy? *Acta Oncol.* **56**, 1522–1530 <https://doi.org/10.1080/0284186X.2017.1348623> (2017).
45. Mao, Y., Poschke, I. & Kiessling, R. Tumour-induced immune suppression: role of inflammatory mediators released by myelomonocytic cells. *J Intern Med.* **276**, 154–170 <https://doi.org/10.1111/joim.12229> (2014).
46. Wculek, S. K. *et al.* Dendritic cells in cancer immunology and immunotherapy. *Nat Rev Immunol.* **20**, 7–24 <https://doi.org/10.1038/s41577-019-0210-z> (2020).
47. Altman, B. J., Stine, Z. E. & Dang, C. V. From Krebs to clinic: glutamine metabolism to cancer therapy. *Nat Rev Cancer.* **16**, 619–634 <https://doi.org/10.1038/nrc.2016.71> (2016).
48. Li, L. *et al.* Transcriptional Regulation of the Warburg Effect in Cancer by SIX1. *Cancer Cell* **33**, 368–385 e367, doi:10.1016/j.ccell.2018.01.010 (2018).
49. Rodriguez-Enriquez, S. *et al.* Transcriptional Regulation of Energy Metabolism in Cancer Cells. *Cells.* **8**, <https://doi.org/10.3390/cells8101225> (2019).
50. Chae, Y. C. *et al.* Mitochondrial Akt Regulation of Hypoxic Tumor Reprogramming. *Cancer Cell.* **30**, 257–272 <https://doi.org/10.1016/j.ccell.2016.07.004> (2016).
51. Park, S. *et al.* Role of the Pyruvate Dehydrogenase Complex in Metabolic Remodeling: Differential Pyruvate Dehydrogenase Complex Functions in Metabolism. *Diabetes Metab J.* **42**, 270–281 <https://doi.org/10.4093/dmj.2018.0101> (2018).
52. Stacpoole, P. W. Therapeutic Targeting of the Pyruvate Dehydrogenase Complex/Pyruvate Dehydrogenase Kinase (PDC/PDK) Axis in Cancer. *J Natl Cancer Inst.* **109**, <https://doi.org/10.1093/jnci/djx071> (2017).
53. Cai, Z. *et al.* Phosphorylation of PDHA by AMPK Drives TCA Cycle to Promote Cancer Metastasis. *Mol Cell* **80**, 263–278 e267, doi:10.1016/j.molcel.2020.09.018 (2020).
54. Wang, Z. & Dong, C. Gluconeogenesis in Cancer: Function and Regulation of PEPCK, FBPase, and G6Pase. *Trends Cancer.* **5**, 30–45 <https://doi.org/10.1016/j.trecan.2018.11.003> (2019).
55. Vyas, S., Zaganjor, E. & Haigis, M. C. Mitochondria and Cancer. *Cell.* **166**, 555–566 <https://doi.org/10.1016/j.cell.2016.07.002> (2016).
56. Hay, N. Reprogramming glucose metabolism in cancer: can it be exploited for cancer therapy? *Nat Rev Cancer.* **16**, 635–649 <https://doi.org/10.1038/nrc.2016.77> (2016).
57. Fane, M. & Weeraratna, A. T. How the ageing microenvironment influences tumour progression. *Nat Rev Cancer.* **20**, 89–106 <https://doi.org/10.1038/s41568-019-0222-9> (2020).
58. Mizrahi, J. D., Surana, R., Valle, J. W. & Shroff, R. T. Pancreatic cancer. *The Lancet.* **395**, 2008–2020 [https://doi.org/10.1016/s0140-6736\(20\)30974-0](https://doi.org/10.1016/s0140-6736(20)30974-0) (2020).

59. Wang, W. *et al.* CD8(+) T cells regulate tumour ferroptosis during cancer immunotherapy. *Nature*. **569**, 270–274 <https://doi.org/10.1038/s41586-019-1170-y> (2019).
60. Chen, D. S. & Mellman, I. Elements of cancer immunity and the cancer-immune set point. *Nature*. **541**, 321–330 <https://doi.org/10.1038/nature21349> (2017).
61. Vago, L. & Gojo, I. Immune escape and immunotherapy of acute myeloid leukemia. *J Clin Invest*. **130**, 1552–1564 <https://doi.org/10.1172/JCI129204> (2020).
62. Miao, Y. *et al.* Adaptive Immune Resistance Emerges from Tumor-Initiating Stem Cells. *Cell* **177**, 1172–1186 e1114, [doi:10.1016/j.cell.2019.03.025](https://doi.org/10.1016/j.cell.2019.03.025) (2019).
63. Leone, R. D. & Powell, J. D. Metabolism of immune cells in cancer. *Nat Rev Cancer*. **20**, 516–531 <https://doi.org/10.1038/s41568-020-0273-y> (2020).
64. Binnewies, M. *et al.* Understanding the tumor immune microenvironment (TIME) for effective therapy. *Nat Med*. **24**, 541–550 <https://doi.org/10.1038/s41591-018-0014-x> (2018).
65. Nagarsheth, N., Wicha, M. S. & Zou, W. Chemokines in the cancer microenvironment and their relevance in cancer immunotherapy. *Nat Rev Immunol*. **17**, 559–572 <https://doi.org/10.1038/nri.2017.49> (2017).
66. Buck, M. D., Sowell, R. T., Kaech, S. M. & Pearce, E. L. *Metabolic Instruction of Immunity*. *Cell*. **169**, 570–586 <https://doi.org/10.1016/j.cell.2017.04.004> (2017).
67. Mehta, M. M., Weinberg, S. E. & Chandel, N. S. Mitochondrial control of immunity: beyond ATP. *Nat Rev Immunol*. **17**, 608–620 <https://doi.org/10.1038/nri.2017.66> (2017).
68. Altorki, N. K. *et al.* The lung microenvironment: an important regulator of tumour growth and metastasis. *Nat Rev Cancer*. **19**, 9–31 <https://doi.org/10.1038/s41568-018-0081-9> (2019).
69. Quail, D. F. & Joyce, J. A. The Microenvironmental Landscape of Brain Tumors. *Cancer Cell*. **31**, 326–341 <https://doi.org/10.1016/j.ccell.2017.02.009> (2017).
70. O'Sullivan, D., Sanin, D. E., Pearce, E. J. & Pearce, E. L. Metabolic interventions in the immune response to cancer. *Nat Rev Immunol*. **19**, 324–335 <https://doi.org/10.1038/s41577-019-0140-9> (2019).
71. Nishida, N. & Kudo, M. Oncogenic Signal and Tumor Microenvironment in Hepatocellular Carcinoma. *Oncology*. **93** (Suppl 1), 160–164 <https://doi.org/10.1159/000481246> (2017).
72. Jiang, H. *et al.* Targeting focal adhesion kinase renders pancreatic cancers responsive to checkpoint immunotherapy. *Nat Med*. **22**, 851–860 <https://doi.org/10.1038/nm.4123> (2016).
73. Wang, Y., Xia, Y. & Lu, Z. Metabolic features of cancer cells. *Cancer Commun (Lond)*. **38**, 65 <https://doi.org/10.1186/s40880-018-0335-7> (2018).
74. Vazquez, A. *et al.* Cancer metabolism at a glance. *J Cell Sci*. **129**, 3367–3373 <https://doi.org/10.1242/jcs.181016> (2016).
75. Loftus, R. M., Finlay, D. K. & Immunometabolism Cellular Metabolism Turns Immune Regulator. *J Biol Chem*. **291**, 1–10 <https://doi.org/10.1074/jbc.R115.693903> (2016).

76. Fesnak, A. D., June, C. H. & Levine, B. L. Engineered T cells: the promise and challenges of cancer immunotherapy. *Nat Rev Cancer*. **16**, 566–581 <https://doi.org/10.1038/nrc.2016.97> (2016).
77. Faubert, B., Solmonson, A. & DeBerardinis, R. J. Metabolic reprogramming and cancer progression. *Science*. **368**, <https://doi.org/10.1126/science.aaw5473> (2020).
78. Gonzalez, H., Hagerling, C. & Werb, Z. Roles of the immune system in cancer: from tumor initiation to metastatic progression. *Genes Dev*. **32**, 1267–1284 <https://doi.org/10.1101/gad.314617.118> (2018).
79. Yang, X., Zhang, Z., Zhang, L. & Zhou, L. MicroRNA hsa-mir-3923 serves as a diagnostic and prognostic biomarker for gastric carcinoma. *Sci Rep*. **10**, 4672 <https://doi.org/10.1038/s41598-020-61633-8> (2020).
80. Zhang, Z., Wang, S., Yang, F., Meng, Z. & Liu, Y. LncRNA ROR1AS1 high expression and its prognostic significance in liver cancer. *Oncol Rep*. **43**, 55–74 <https://doi.org/10.3892/or.2019.7398> (2020).
81. Subramanian, A. *et al.* Gene set enrichment analysis: a knowledge-based approach for interpreting genome-wide expression profiles. *Proc Natl Acad Sci U S A*. **102**, 15545–15550 <https://doi.org/10.1073/pnas.0506580102> (2005).
82. Priestley, P. *et al.* Pan-cancer whole-genome analyses of metastatic solid tumours. *Nature*. **575**, 210–216 <https://doi.org/10.1038/s41586-019-1689-y> (2019).
83. Robinson, M. D., McCarthy, D. J. & Smyth, G. K. edgeR: a Bioconductor package for differential expression analysis of digital gene expression data. *Bioinformatics*. **26**, 139–140 <https://doi.org/10.1093/bioinformatics/btp616> (2010).
84. Kourou, K., Exarchos, T. P., Exarchos, K. P., Karamouzis, M. V. & Fotiadis D. I. Machine learning applications in cancer prognosis and prediction. *Comput Struct Biotechnol J*. **13**, 8–17 <https://doi.org/10.1016/j.csbj.2014.11.005> (2015).
85. Robin, X. *et al.* pROC: an open-source package for R and S + to analyze and compare ROC curves. *BMC Bioinformatics*. **12**, 77 <https://doi.org/10.1186/1471-2105-12-77> (2011).
86. Lin, H. & Zelterman, D. Modeling Survival Data: Extending the Cox Model. *Technometrics*. **44**, 85–86 <https://doi.org/10.1198/tech.2002.s656> (2002).
87. Chen, L. *et al.* Identification of biomarkers associated with diagnosis and prognosis of colorectal cancer patients based on integrated bioinformatics analysis. *Gene*. **692**, 119–125 <https://doi.org/10.1016/j.gene.2019.01.001> (2019).
88. Newman, A. M. *et al.* Robust enumeration of cell subsets from tissue expression profiles. *Nat Methods*. **12**, 453–457 <https://doi.org/10.1038/nmeth.3337> (2015).
89. Gentles, A. J. *et al.* The prognostic landscape of genes and infiltrating immune cells across human cancers. *Nat Med*. **21**, 938–945 <https://doi.org/10.1038/nm.3909> (2015).
90. Yu, X., Chen, Y. A., Conejo-Garcia, J. R., Chung, C. H. & Wang, X. Estimation of immune cell content in tumor using single-cell RNA-seq reference data. *BMC Cancer*. **19**, 715 <https://doi.org/10.1186/s12885-019-5927-3> (2019).

91. Thorsson, V. *et al.* The Immune Landscape of Cancer. *Immunity* **48**, 812–830 e814, doi:10.1016/j.immuni.2018.03.023 (2018).

92. Li, T. *et al.* TIMER: A Web Server for Comprehensive Analysis of Tumor-Infiltrating Immune Cells. *Cancer Res.* **77**, e108–e110 <https://doi.org/10.1158/0008-5472.CAN-17-0307> (2017).

93. Reinhold, W. C. *et al.* RNA Sequencing of the NCI-60: Integration into CellMiner and CellMiner CDB. *Cancer Res.* **79**, 3514–3524 <https://doi.org/10.1158/0008-5472.CAN-18-2047> (2019).

Figures

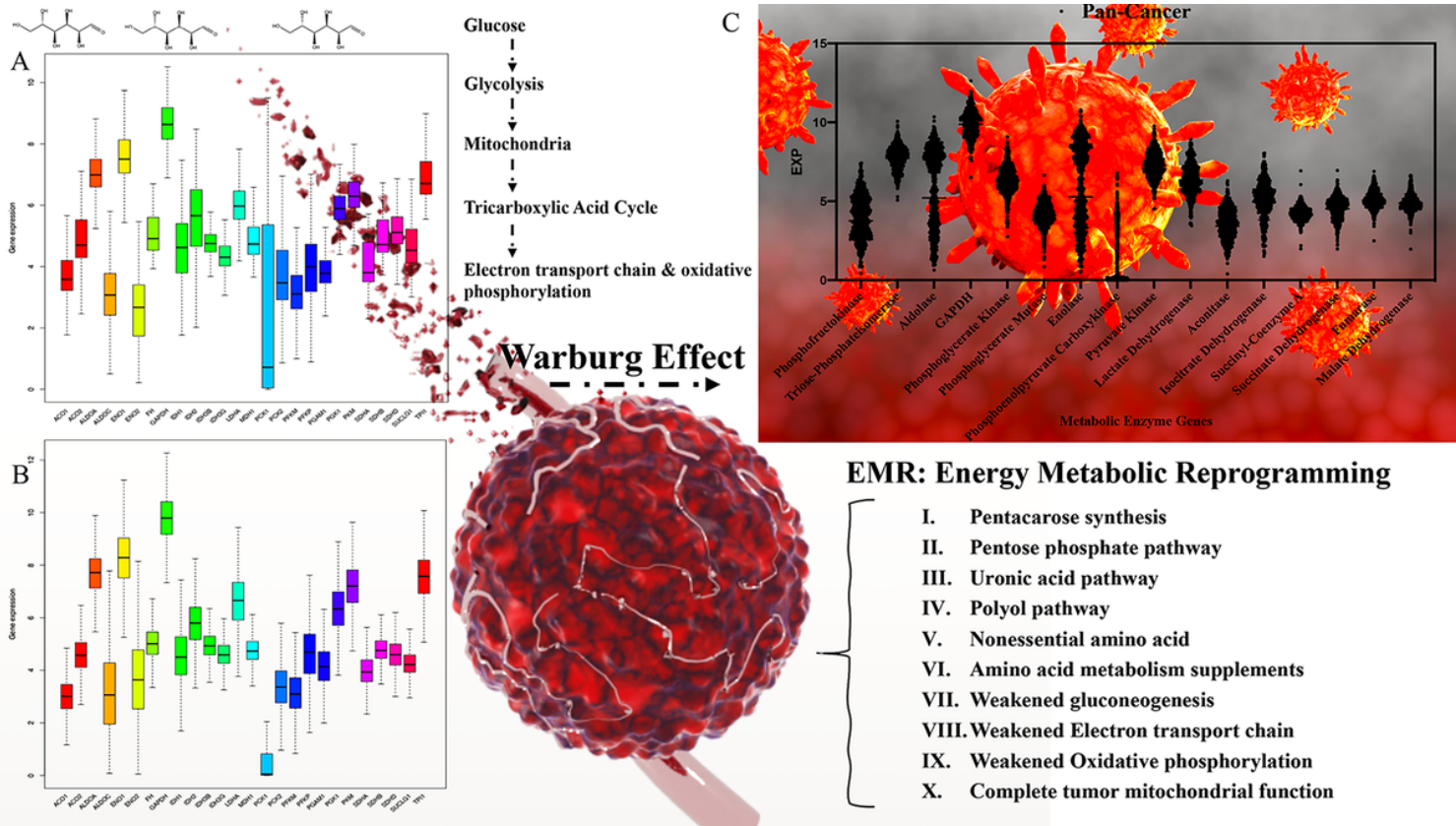


Figure 1

The expression differences of metabolic enzyme coding genes in different tissues (A) Average mRNA expression level of metabolic enzyme coding genes in normal cells. (B) Average mRNA expression level of metabolic enzyme coding genes in tumor cells. (C) Average mRNA expression level of Pan-cancer metabolic enzymes. The phenomenon that there were tremendous fluctuations in the component percentage of enzyme genes associated with glycolysis in tumor cells. Even after adjustment, there still existed a broad range of differences in some enzyme gene expression between not only distinct clinical stages in the same tumor but also different tumor types. Specifically, the fluctuations of the three enzymes, phosphofructokinase, aldolase, and enolase respectively encoded by PFKM, ALDOC, and ENO1/2 were most prominent, indirectly reflecting a stronger perception and ability of tumor cells in response to energy state disturbance. The cascade amplification of glucose metabolic flux is affected by

the blocking effect of PCK/PEPCK, together with the structurally stable expression of GAPDH, phosphoglycerate kinase and phosphoglycerate mutase.

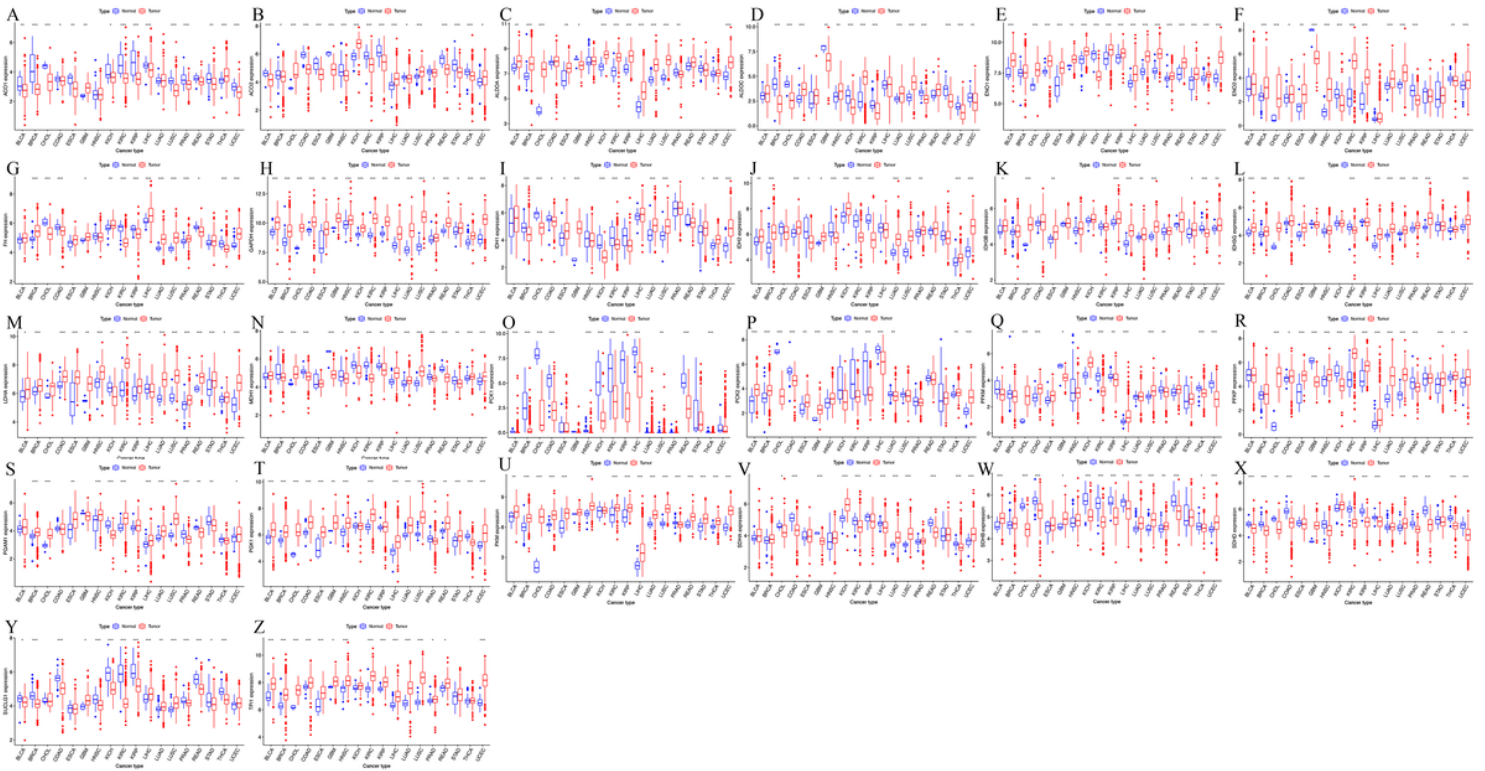


Figure 2

Metabolic enzymes coding genes across 18 solid cancers In the tumors from the microenvironment with sufficient blood supply and abundant glucose and oxygen contents, for example, a liver-derived tumor, kidney-derived tumors, and lung-derived, glucose uptaken by tumor cells can fast enter the pentose phosphate pathway, providing the sources of pentose sugars and synchronously ensuring that part of glucose is split into pyruvate in glycolytic metabolism, followed by the entry of pyruvate into the TCA cycle for ATP synthesis. However, a fast transformation of glucose to lactic acids only exists in high-grade tumors. Obviously, in tumors of low-grade origins like LIHC and KICH, the transformation of glucose to lactic acids is not vibrant. This may relate to the biological behavior, i.e., expansive growth, at the early stage of multiple low-grade tumors, including the two types. Consequently, regional LDHA enzyme expression and lactic acid contents reflect the tumor grade to some extent. As for tumors derived from the microenvironment with sufficient blood supply and glucose and oxygen contents, they will select glucose metabolic flux toward either glycolysis or the TCA cycle. Similar to CHOL, COAD, STES, and UCEC, although intermediate products also support the syntheses of macromolecules except for ATP during glycolysis, only a small amount of glucose flows to the alternative pathways^{6,58,59}. Additionally, more glucose flows to the mitochondria to ensure ATP synthesis⁶⁰. Such an alternation of metabolic flux benefits in situ proliferation and growth of tumor cells, which can also be found in the main biological behavior of invasive and extensive growth in these tumors at the early stage. Finally, in terms of tumors in the microenvironment with insufficient blood supply and glucose and oxygen contents, for instance, GBM, the original metabolic pattern is almost completely changed. Briefly, high-grade tumors often have a low

flux of alternative pathways of glucose metabolism, although it contradicts with the high proliferation, such a shift of metabolic flux can alter the tumor microenvironment through the transformation of pyruvic acids to lactic acids via lactic dehydrogenase, low oxidation-reduction levels, high glycolytic activity, and lactic acid generation, resulting in acid and anoxic tumor environment.

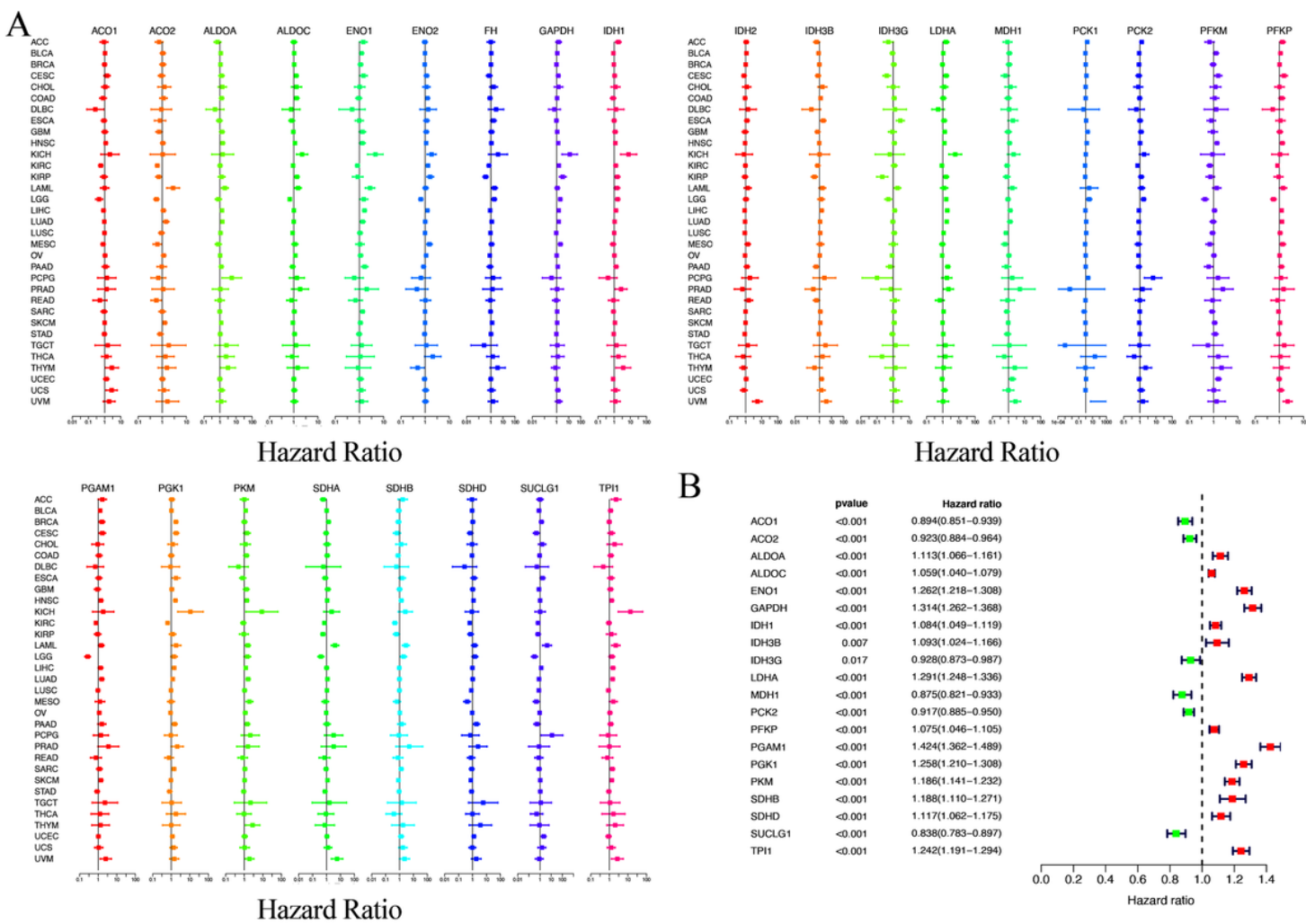


Figure 3

Cox analysis for the assessment of the predictive effect on OS and the relapse-free survival. As gene markers, the selected 26 genes encoding metabolic enzymes were reversely labeled into 33 tumors from the database to plot hazard ratios of different genes encoding metabolic enzymes for each tumor patient. Using the COX tool in “p-ROC package” to analyses the results of multivariate survival for pan-cancers. Forest plots showing log2 hazard ratio (95% confidence interval). Adjusted $p < 0.05$.

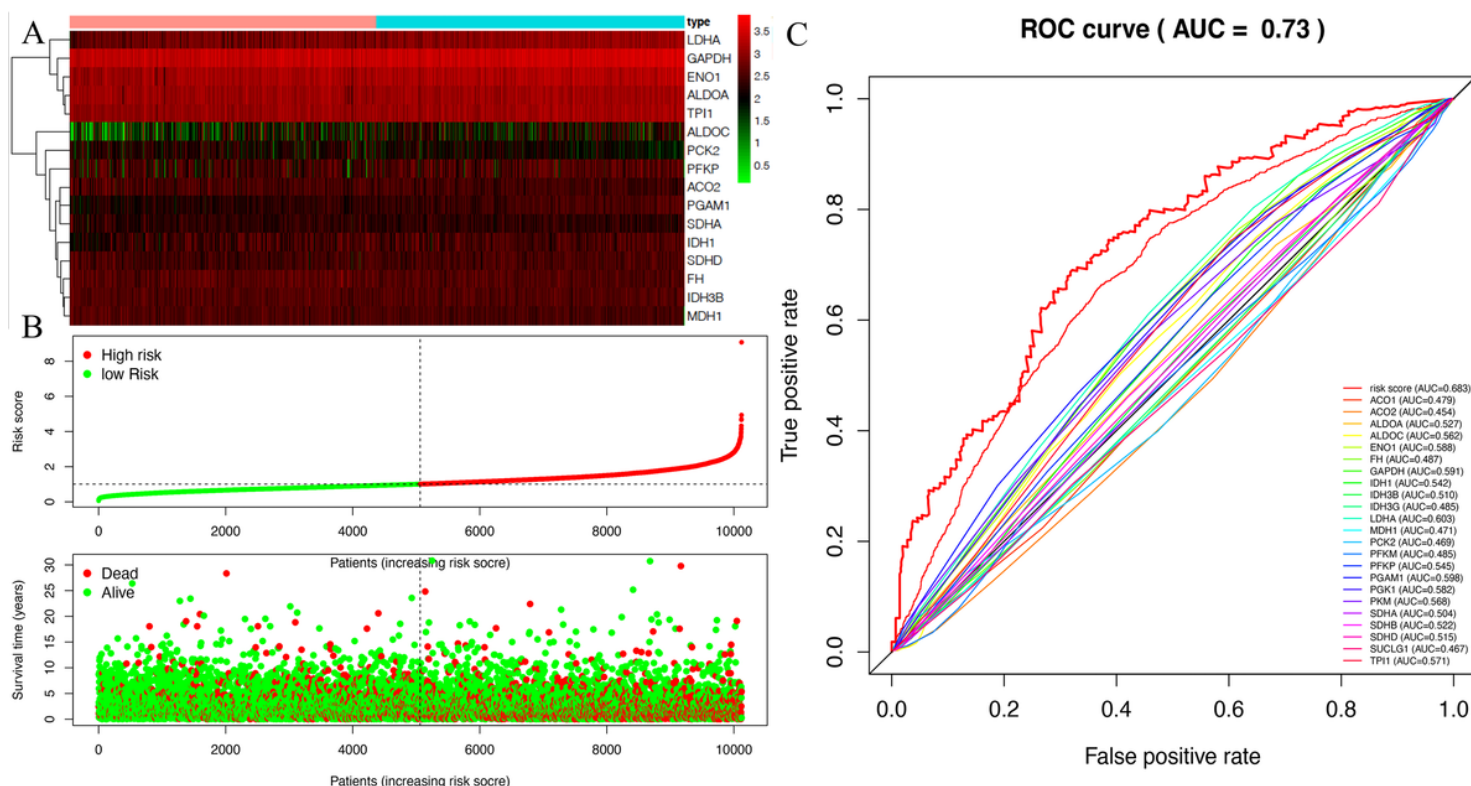


Figure 4

Risk score and ROC curves. (A) 16 metabolic enzymes in the glucose metabolic profiles affecting the prognosis of patients were assessed. (B) Based on the hazard ratios, patients were stratified into the high-risk group and the low-risk group. With a mortality rate of 55.15%, the high-risk group was at a higher risk of death. The mortality of the low-risk group was 37.13%. The Chi-square test showed a significant difference in mortality between the two groups ($p < 0.05$). (C) ROC curves were plotted, and the mean AUC was 0.683 ($P < 0.05$). Besides, we also used ROC curve analysis to compare survival prediction values based on mRNA expression traits of all glucose metabolic enzymes profiles. After we excluded enzymes with low survival prediction values ($AUC < 0.5$) and only retained those with an $AUC > 0.5$, the mean AUC of ROC curves was 0.73. ($P < 0.01$) Abbreviations: AUC, area under the curve; ROC, receiver-operating characteristic curve.

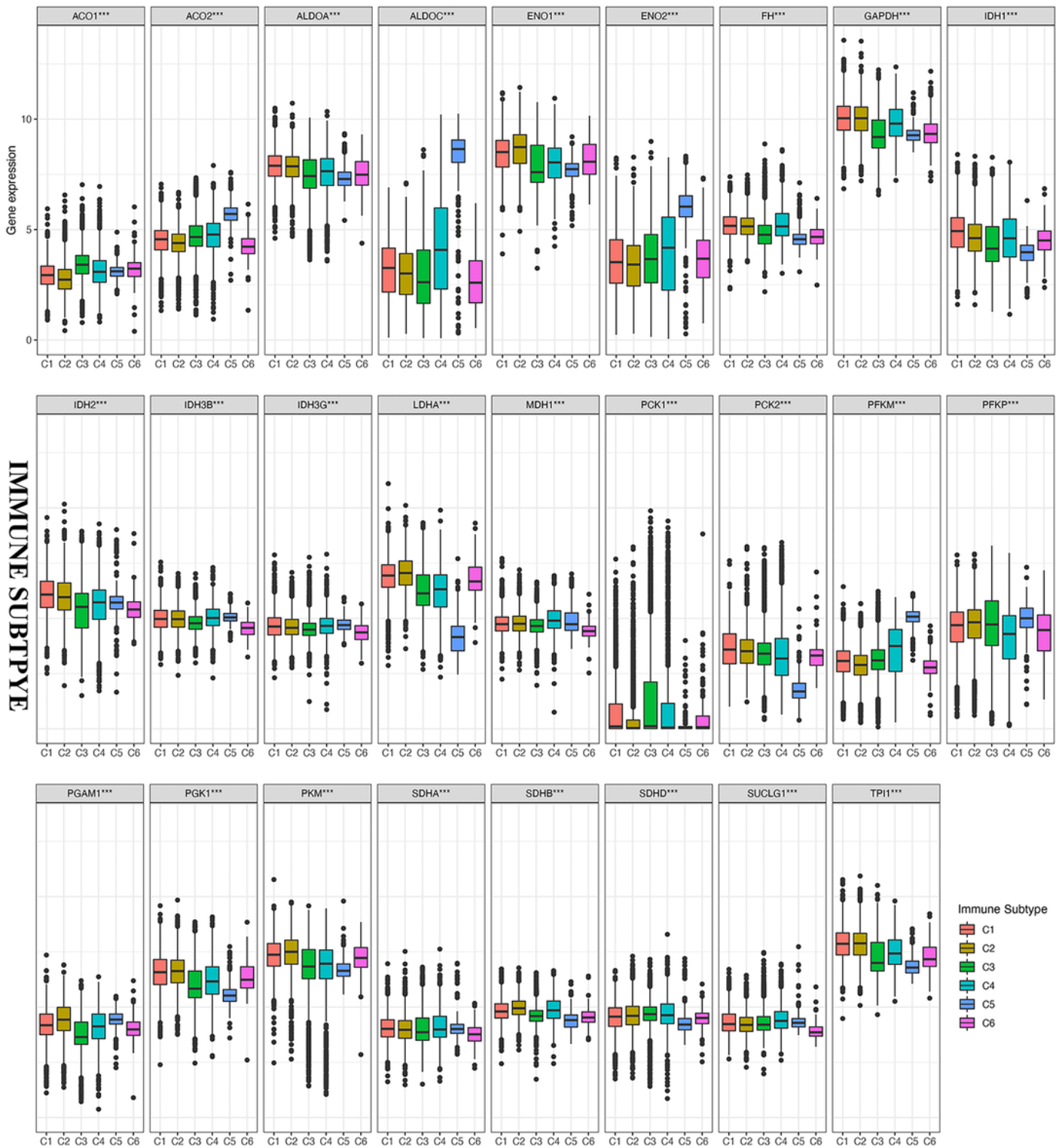


Figure 5

The analysis results of immune subtypes. The result showed that in six different subtypes C1-6 (C1: wound healing, C2: IFN-g dominant, C3: inflammatory, C4: lymphocyte depleted, C5: immunologically quiet, and C6: TGF- β dominant), there existed strong associations between all of the 26 enzyme-encoding genes in the pan-cancer glucose metabolic pathways and immune subtypes. Note: * $p < 0.05$, ** $p < 0.01$, *** $p < 0.001$.

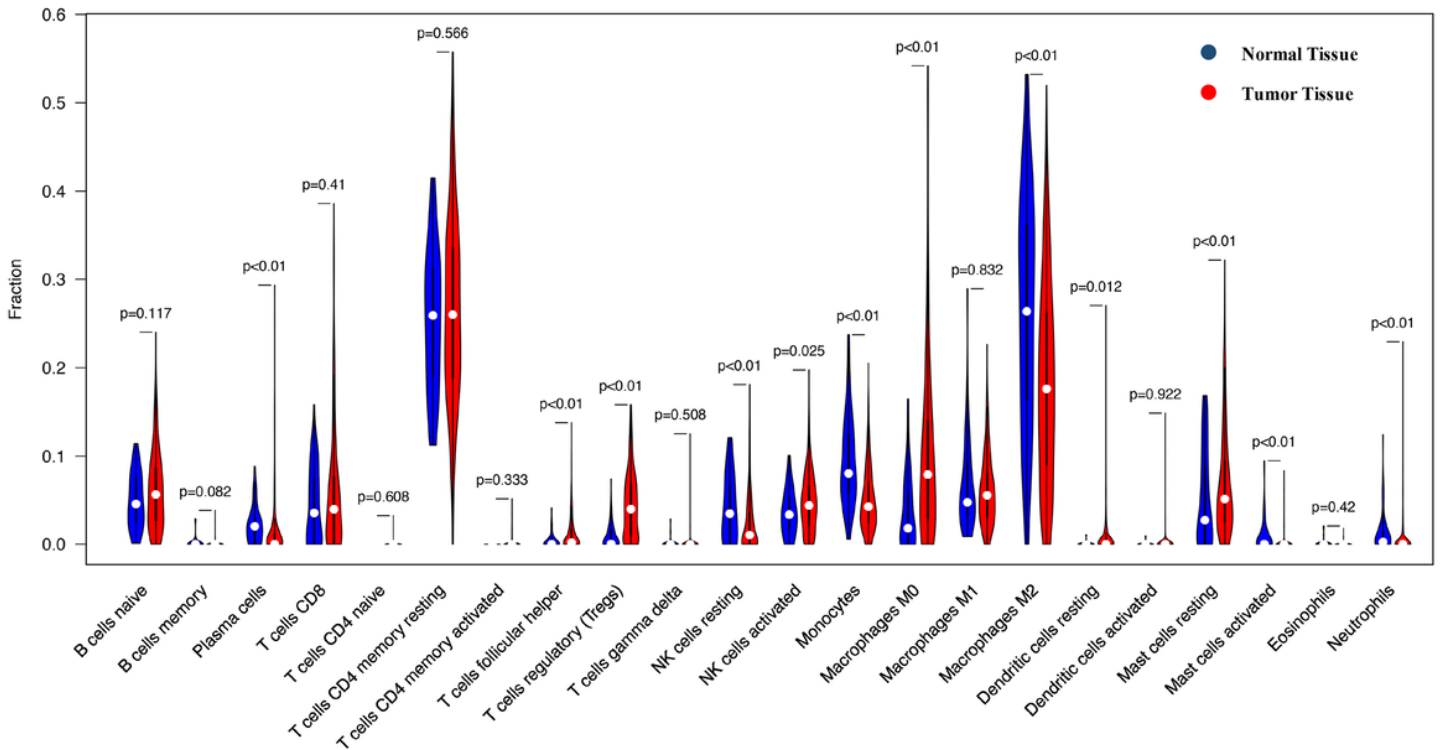


Figure 6

The different proportions of distinct immune cells in the pan-cancer immune microenvironment. Subpopulations of immune cells with high metabolic activity can lead to regional nutrient consumption, hypoxia, acidity, and metabolite accumulation in the TME, finally resulting in the establishment of metabolic competition between cancer cells and immune cells. As indicated from the proportions of distinct immune cells in the pan-cancer immune microenvironment, the effector cells that mediated the acquired immunity, including plasma cells ($p < 0.01$), resting natural killer (NK) cells ($p < 0.01$), monocytes ($p < 0.01$), M2 macrophages ($p < 0.01$), activated mast cells ($p < 0.01$), and neutrophils ($p < 0.01$), showed low proportions. By contrast, T follicular helper cells ($p < 0.01$), T regulatory cells (Tregs) ($p < 0.01$), activated natural killer (NK) cells ($p = 0.025$), M0 macrophages ($p < 0.01$), resting dendritic cells ($p = 0.012$) and resting mast cells ($p < 0.01$) those who mediated the congenital immunity, exhibited a significantly weaker killing effect on tumor cells than those that mediated the humoral and cellular immune responses, regardless of their high expression levels.

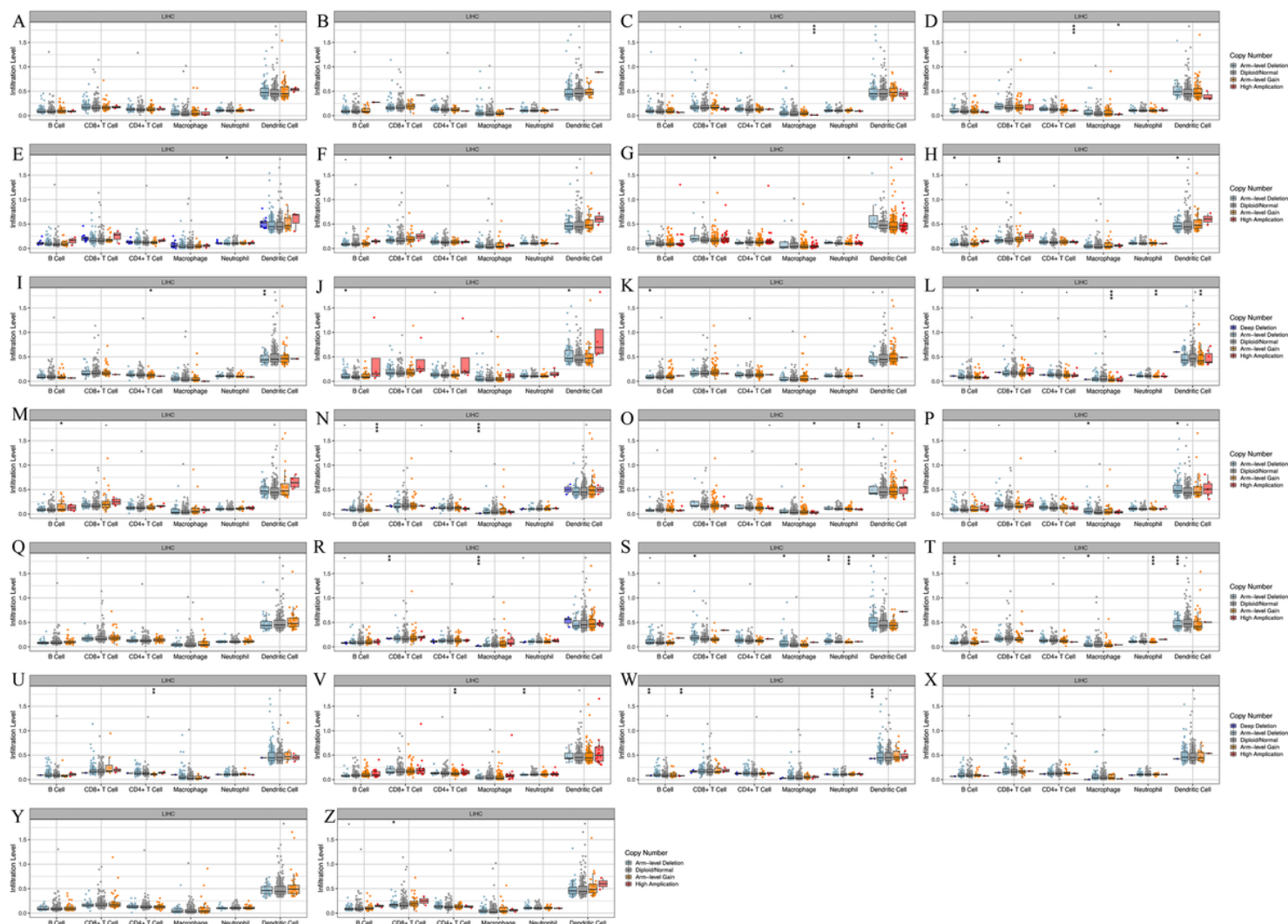


Figure 7

Correlation analysis of immune cell metabolism pathways. Six representative immune cells (B cells, CD8+ T cells, CD4+ T cells, macrophages, neutrophils, and dendritic cells) in LIHC to analyze associations between genes encoding glucose metabolic enzymes. Note: * $p < 0.05$, ** $p < 0.01$, *** $p < 0.001$. Note: A.ACO1 B.ACO2 C.ALDOA D.ALDOC E.ENO1 F.ENO2 G.FH H.GAPDH I.IDH1 J.IDH2 K.IDH3B L.IDH3G M.LDHA N.MDH1 O.PCK1 P.PCK2 Q.PFKM R.PFKP S.PGAM1 T.PGK1 U.PKM V.SDHA W.SDHB X.SDHD Y.SUCLG1 Z.TPI1.

synthesis of pentose sugars, satisfying the high glucose uptake in aerobic glycolysis and metabolism and thereby promoting biosynthesis in tumor cells. The results demonstrate that the change of glucose metabolism flow in tumor tissue may not only be the independent action of certain enzymes, but also the synergistic effect of certain enzymes.

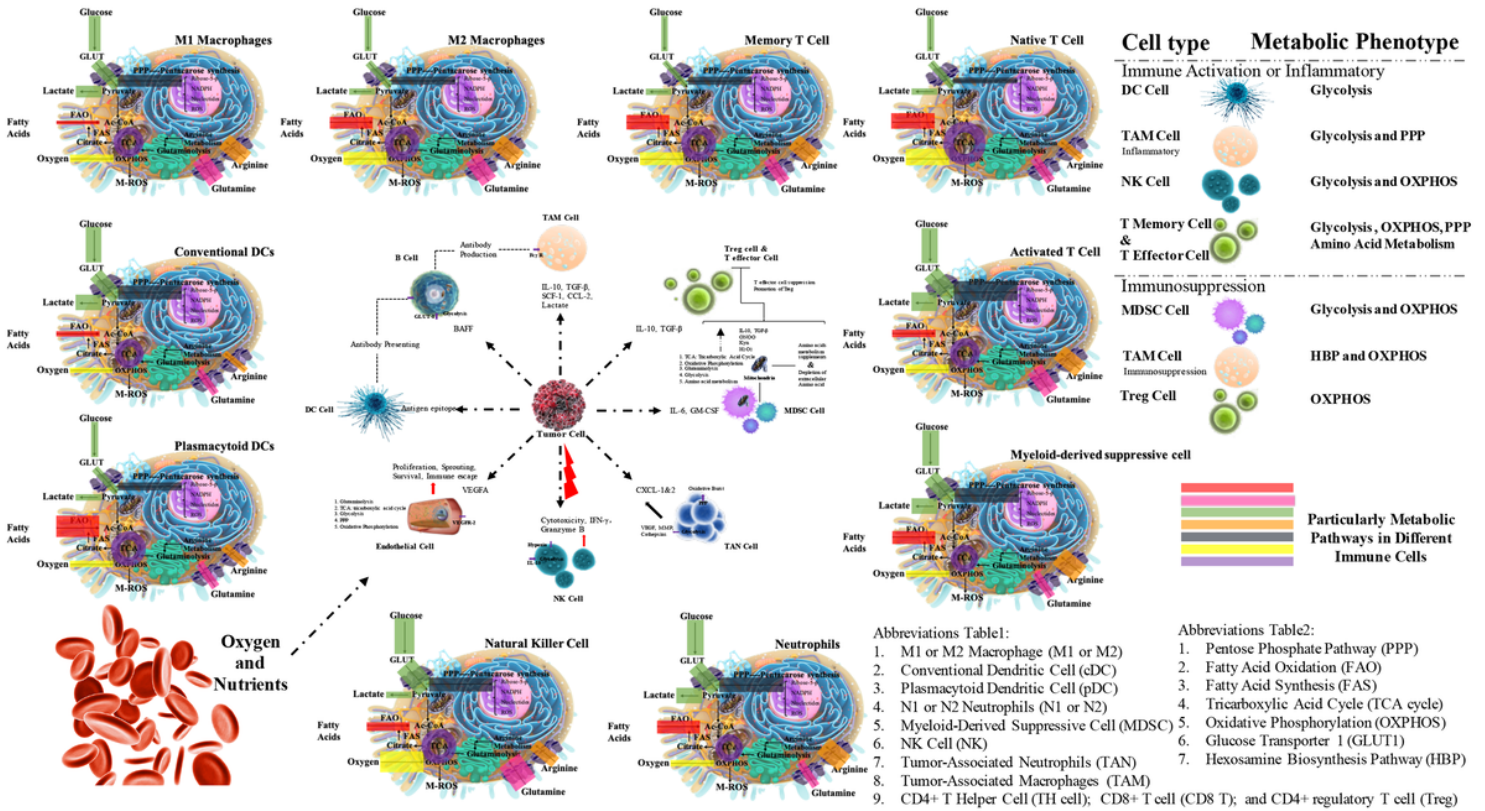


Figure 9

Metabolic Instruction of Different Immunity Cells. Metabolic reprogramming of immune cells in the pan-cancer immune microenvironment. Metabolic reprogramming of immune cells in the cancer-associated immune microenvironment. In the tumor microenvironment (TME), regional hypoxia, low pH, loss of collagenase resulting from structural changes in the expression profiles of metabolic enzymes are even accompanied by the dual effect of immunosuppression and/or “cancer immunoediting” that facilitates tumor growth. The Figure indicated that multiple immune effector cells might share similar metabolic pathways with tumor cells in the TME. Interestingly, the process of immune cell activation is accompanied by the “adaptive reassortment of glucose metabolism”, and the distinctive “metabolic adaptive reassortment” in immune cells is regarded as a critical trait of immune cell activation by a large number of researchers.